Journal of Materials Chemistry

Cite this: *J. Mater. Chem.*, 2012, **22**, 7449

www.rsc.org/materials

PAPER

Metal–organic framework MIL-100(Fe) for the adsorption of malachite green from aqueous solution†

Shu-Hui Huo and Xiu-Ping Yan*

Received 10th December 2011, Accepted 6th February 2012
DOI: 10.1039/c2jm16513a

The adsorption of malachite green from aqueous solution on a highly porous metal–organic framework MIL-100(Fe) was studied in view of the adsorption isotherm, thermodynamics, kinetics, and regeneration of the sorbent. The adsorption isotherms of malachite green on MIL-100(Fe) followed the Freundlich model, and MIL-100(Fe) possessed heterogeneous surface caused by the presence of different functional groups on the surface. The adsorption of malachite green on MIL-100(Fe) is controlled by an entropy effect rather than an enthalpy change, and obeyed a pseudo-second-order kinetics. Analysis of the intraparticle diffusion plots revealed that more than one process affected the adsorption, and film (boundary layer) diffusion controlled the adsorption rate at the beginning. Evidence from zeta potential and X-ray photoelectron spectroscopic data showed that the adsorption of malachite green was also driven by electrostatic attraction and the interaction between the Lewis base $-N(CH_3)_2$ in malachite green and the water molecule coordinated metal sites of MIL-100(Fe). MIL-100(Fe) gave much higher adsorption capacity for malachite green than other conventional adsorbents such as activated carbon and natural zeolite. The high adsorption capacity, good solvent stability, and excellent reusability make MIL-100(Fe) attractive for the removal of MG from aqueous solution.

Introduction

Metal–organic frameworks (MOFs) are an intriguing class of highly porous hybrid materials constructed by metal-containing nodes connected by various organic bridges, which bear multiple complexing functions.[1–4] Compared with conventional adsorbents, the merits of MOFs as adsorbents are their diverse compositions and structure types, tunable pore size, large surface area, and coordinatively unsaturated or saturated metal sites to regulate the adsorption ability.[5–7] MOFs have been shown great potential in sorption-related fields.[5–22] Up to now, MOFs have been widely explored for gas storage of H_2,[8] capture of greenhouse gases,[9] and adsorption of volatile organic compounds.[10,11] Moreover, the adsorption and removal of pharmaceuticals (furosemide and sulfasalazine),[12] dyes,[13,14] alkylaromatics and phenols,[15–18] and sulfur compounds[19–22] from liquid phase have also been reported. Nevertheless, research on aqueous adsorption of contaminants on MOFs is limited though such studies will pave the way to wide application of MOFs in removal and adsorption of contaminants from polluted aqueous environment.

As a cationic triphenylmethane dye, MG exists extensively in wastewaters from textile, leather tanning, and paper production industries.[23,24] MG has also been used in aquaculture illicitly which aggravates water pollution and causes great environment concern.[25] MG contaminant not only deteriorates water quality, but also makes a significant impact on human health due to toxic, carcinogenic, mutagenic or teratogenic effects. Therefore, the removal of malachite green from contaminated water has attracted much attention because of its detrimental effects on both ecological environment and human health.[25,26]

To date, various methods have been developed to remove MG from aqueous solution, including photodegradation,[27] biodegradation,[28] and adsorption.[24,29] The adsorption method is attractive for the removal of dyes because dyes are not only moderately stable to light and heat, but also resistant to oxidation and biodegradation. Besides, the adsorption technique works effectively without the need for additional pretreatment before its application. Activated carbons and zeolites are well-studied classes of materials for the adsorption of MG from water.[30–33] Though activated carbon has been used widely as a potential adsorbent for the adsorption and removal of MG, the adsorption capacity is quite limited.[30,31,34] Thus, it is still of great significance to discover new materials for efficient adsorption and removal of MG.

Here we report the adsorption and removal of malachite green (MG) from aqueous solution on MOF MIL-100(Fe)

State Key Laboratory of Medicinal Chemical Biology, and Research Center for Analytical Sciences, College of Chemistry, Nankai University, Tianjin 300071, China. E-mail: xpyan@nankai.edu.cn; Fax: +86 22-23506075; Tel: +86 22-23506075

† Electronic supplementary information (ESI) available. See DOI: 10.1039/c2jm16513a

$(Fe_3F(H_2O)_2O[C_6H_3(CO_2)_3]_2 \cdot nH_2O)$. MIL-100(Fe) is built up from carboxylate moieties (benzene-1,3,5-tricarboxylate (BTC)) and iron trimeric octahedral clusters which have removable terminal ligands (H_2O, F, or OH) and therefore provide potential unsaturated metal sites for strong interaction.[35,36] MOF-100(Fe) also has two types of large accessible and permanent pores (25 Å and 29 Å in diameter) with microporous windows (5.5 Å and 8.6 Å in diameter).[35] In this work, the adsorption of MG on MIL-100(Fe) was studied in respect of adsorption isotherm, thermodynamics and kinetics. Activated carbon, MOF MIL-101(Cr) and MIL-53(Al) were also used for comparison to demonstrate the superior adsorption capacity of MIL-100(Fe) in the overall sorption of MG.

Experimental

Chemicals and materials

All chemicals used were at least of analytical grade. Nitric acid (Guangfu, Tianjin, China), hydrofluoric acid, iron powder, and 1,3,5-benzenetricarboxylic acid (trimesic acid, H_3BTC) (Aladdin, Shanghai, China) were used to prepare MIL-100(Fe). $Al(NO_3)_3 \cdot 9H_2O$ and terephthalic acid (Aladdin, Shanghai, China) were used to prepare MIL-53. $Cr(NO_3)_3 \cdot 9H_2O$ (Sinopharm, Shanghai, China) and terephthalic acid and hydrofluoric acid were used to prepare MIL-101. MIL-53, MIL-101 and activated carbon (Beifang Tianyi, Tianjin, China) were also used as adsorbents for comparison. Ethanol and *N*,*N*-dimethylformamide (DMF) (Guangfu, Tianjin, China) were used for washing and purification. Ultrapure water (18.2 MΩ cm) was obtained from a WaterPro Water Purification System (Labconco Corporation, Kansas City, MO, USA). A stock solution of MG (1000 mg L^{-1}) was prepared by dissolving solid MG in ultrapure water, and kept at 4 °C in the dark. Working solutions of MG were prepared by step-by-step dilution of the stock solution with ultrapure water before use. **Caution**: Take care to avoid direct contact with MG because of its toxicity, and quick coloration on skin and irritation to skin, eyes and respiratory tract.

Characterization of the MOFs

The X-ray diffraction (XRD) patterns were recorded with a D/max-2500 diffractometer (Rigaku, Japan) using Cu K_α radiation ($\lambda = 1.5418$ Å) over the angular range from 3° to 80°. The surface area, pore volume, and pore size distributions of adsorbents were measured on a NOVA 2000e surface area and pore size analyzer (Quantachrome, Florida, FL, USA) at 77 K in the range $0.02 \leq P/P_0 \leq 0.20$. The Barrett–Joyner–Halenda (BJH) method was used to calculate the mesopore distribution for the adsorbents. The morphology of MIL-100(Fe) was characterized on a Nova Nano SEM 430 field emission gun scanning electron microscope (FEI, Hillsboro, Oregon, USA). Thermogravimetric analysis (TGA) of MIL-100(Fe) was performed on a PTC-10A thermal gravimetric analyzer (Rigaku, Japan) from room temperature to 800 °C at a ramp rate of 10 °C min^{-1}. Zeta potentials of the adsorbent in ultrapure water were measured on a zeta potential analyzer (Brookhaven Instruments Co., Holtsville, NY, USA). The X-ray photoelectron spectroscopy (XPS) measurements were carried out on a Kratos Axis Ultra DLD spectrometer fitted with a monochromated Al K_α X-ray source ($h\nu$ = 1486.6 ev), hybrid (magnetic/electrostatic) optics, and a multichannel plate and delay line detector (Kratos, Manchester, UK). The ultrasonic device used was a KQ2200E instrument with a frequency of 40 kHz and a nominal power of 80 W (Kunshan, China).

Preparation of the MOFs

MIL-100(Fe) was synthesized according to Yoon *et al.*[36] Briefly, iron powder (277.5 mg), H_3BTC (687.5 mg), hydrofluoric acid (35%, 200 μL), and nitric acid (65%, 190 μL) were well mixed with ultrapure water (20 mL) in a Teflon lined steel autoclave. The autoclave was then placed in an oven at 150 °C for 12 h. After cooling, the light orange solid product was collected by filtration, and washed with ultrapure water. The as-synthesized MIL-100(Fe) was further purified with boiling water at 80 °C for 5 h to remove residual unreacted ions, and then with hot ethanol at 60 °C for 3 h until no detection of colored impurities in the mother liquor solution. The highly purified MIL-100(Fe) was then collected by centrifugation at 10 000 rpm for 10 min. The solid was finally dried at 80 °C under vacuum overnight. The synthesis of MIL-53 and MIL-101 is described in the ESI†.

Adsorption experiments

The adsorbents including MIL-100(Fe), MIL-53(Al), MIL-101(Cr) and activated carbon were dried overnight at 150 °C before use. The aqueous solution of 0.01 M NaCl containing MG at a desired concentration was pre-adjusted for pH with NaOH and HCl. To initiate the experiments, a 10 mL vial equipped with Telflon-lined screw cap received a weighed amount of adsorbent (10.0 ± 0.2 mg), followed by adding 5 mL of MG solution (25–1000 mg L^{-1}) at a controlled temperature. For a kinetic study, the adsorption was carried out at constant temperature, and the supernatant was collected at different time intervals for the determination of unadsorbed MG.

For a thermodynamic study, the static adsorption proceeded for 72 h to reach apparent adsorption equilibrium at different temperatures (25–50 °C). Control experiments were preformed with blanks containing no MG under the same conditions as for the MG solution. Each data point was run in triplicate. All the samples were centrifuged at 10 000 rpm for 5 min and analyzed for the concentration of residual MG using a double beam model UV 3600 spectrophotometer (Shimadzu, Japan) at the calibrated maximum wavelength (λ_{max}) of 617 nm.

Desorption experiments

The feasibility for regenerating the exhausted MIL-100(Fe) saturated with MG was evaluated using the solvent desorption technique. Solutions of $CaCl_2$ (1.0 mol L^{-1}), HCl (0.01 mol L^{-1}), absolute ethanol, and ethanol including HCl (0.5%, v/v) were tested as the eluent to regenerate MIL-100(Fe). For a desorption study, the eluent solution (25 mL) was added to the used MIL-100(Fe) (10.0 mg) in a vial, then the mixture was ultrasonicated at 80 W from 0.5 h to 4 h.

Results and discussion

Characterization of the prepared MIL-100(Fe)

The prepared MIL-100(Fe) was characterized by XRD, TGA, SEM, and N_2 adsorption–desorption experiment (Fig. 1). The experimental XRD pattern of the synthesized MIL-100(Fe) is in good agreement with the simulated one, showing the successful preparation of MIL-100(Fe). The prepared MIL-100(Fe) gave a BET surface area of 1626 $m^2 g^{-1}$ with a pore volume of 0.79 $cm^3 g^{-1}$. The pore size distribution of MIL-100(Fe) estimated by using the Barrett–Joyner–Halenda method gave a pore diameter of maxima at 31.6 Å, which is slightly larger than the large pore (29 Å) of MIL-100(Fe) obtained from the crystal structure.[35] The TGA data reveal that the MIL-100(Fe) is stable up to 330 °C.

Effect of pH on the adsorption of MG

The solution pH may affect the surface charge of MIL-100(Fe), the stability and ionization degree of MG in the solution. Fig. 2 shows the effect of pH on the adsorption of MG on MIL-100(Fe). The adsorption capacity of MIL-100(Fe) for MG increased as the pH increased from 1 to 4, then leveled off in the pH range of 4 to 7, and decreased with further increase of pH from 7 to 10. MG (pK_a 10.3) is protonated in acidic medium and deprotonated at higher pH.[29,37] As the solution pH increased from 1 to 5, the negative charges on the surface of MIL-100(Fe) increased, *i.e.* more negative zeta potential, which was favorable for the adsorption of positively charged MG due to electrostatic attraction. A significant decrease of the adsorption capacity of MIL-100(Fe) for MG in the pH range of 8–10 likely resulted from the instability of MG[38] and the decrease of negative charges on the surface of MIL-100(Fe) (less negative zeta potential) (Fig. 2). Therefore, all other experiments were carried out at pH 5.0.

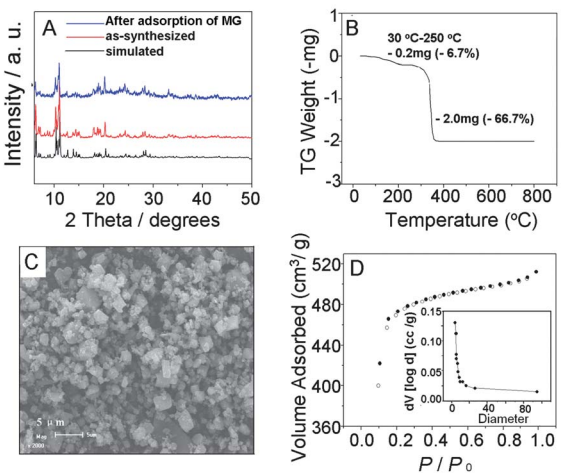

Fig. 1 Characterization of the prepared MIL-100(Fe): (A) comparison of XRD pattern of the as-synthesized MIL-100(Fe) with those simulated and of MG-adsorbed MIL-100(Fe); (B) TGA curve of the as-synthesized MIL-100(Fe); (C) SEM image of the as-synthesized MIL-100(Fe); and (D) N_2 adsorption–desorption isotherms and the pore size distribution of the as-synthesized MIL-100 (inset).

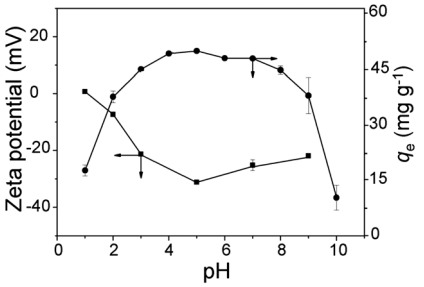

Fig. 2 Effect of pH on the adsorption of MG (100 mg L^{-1}) on MIL-100(Fe) (10.0 mg) containing 0.01 M NaCl, and the zeta potential of MIL-100(Fe) (0.4 mg L^{-1}) at 30 °C.

Effect of ionic strength

Generally, various salts and metal ions exist in dye-containing wastewater. The salts lead to high ionic strength, which may affect the dye adsorption onto adsorbents. The effect of the concentration of NaCl and $CaCl_2$ on the adsorption of MG on MIL-100(Fe) is shown in Fig. S1 (ESI†). The adsorbed capacity of MIL-100(Fe) for MG suddenly dropped once 0.01 mol L^{-1} NaCl or $CaCl_2$ was added. Furthermore, the divalent electrolyte ($CaCl_2$) had more negative effect on the adsorption of MG than the univalent electrolyte (NaCl). However, such a negative effect became negligible as the concentration of NaCl or $CaCl_2$ further increased to 0.1 mol L^{-1}. The above results indicate that electrostatic interaction is one of the mechanisms for the adsorption of MG on MIL-100(Fe).

Adsorption isotherms for MG on MIL-100(Fe)

The adsorption isotherms of MG on MIL-100(Fe) were measured at six different temperatures (Fig. 3A). The Freundlich

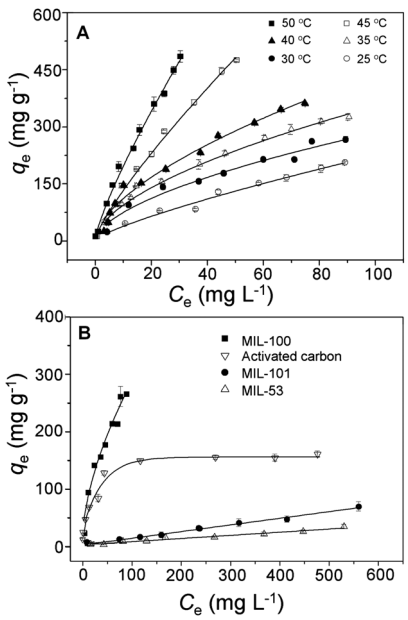

Fig. 3 (A) Adsorption isotherms for MG on MIL-100(Fe) at different temperatures and pH 5.0; (B) adsorption isotherms for MG on different adsorbents at 30 °C and pH 5.0. Solid lines refer to the fitted adsorption isotherms for MOFs by the Freundlich equation, and for activated carbon by the Langmuir equation.

Table 1 Characteristic parameters for the adsorption of MG on MIL-100(Fe)[a]

		Freundlich constants						
T/°C	q_{exp}/mg g^{-1}	1/n	K_F	R^2	ln K_0	ΔG^0/kJ mol^{-1}	ΔH^0/kJ mol^{-1}	ΔS^0/J mol^{-1} K^{-1}
25	205	0.768 ± 0.052	6.49 ± 0.47	0.994	0.93	−2.31	14.5	57.0
30	266	0.580 ± 0.057	12.6 ± 4.65	0.993	1.21	−3.05		
35	325	0.579 ± 0.033	20.6 ± 3.38	0.977	1.24	−3.18		
40	361	0.609 ± 0.038	24.7 ± 3.88	0.963	1.33	−3.48		
45	475	0.805 ± 0.031	26.4 ± 2.28	0.982	1.37	−3.64		
50	485	0.809 ± 0.031	33.5 ± 2.88	0.976	1.44	−3.87		

[a] q_{exp}, experimental adsorption capacity.

isotherm model, which is widely used to describe the adsorption on heterogeneous surfaces caused by the presence of different functional groups on the surface and several adsorbent–adsorbate interactions,[34] was tested to fit the data of MG adsorption isotherm (eqn (1)):

$$q_e = K_F C_e^{1/n} \quad (1)$$

where q_e is the equilibrium adsorption capacity of MG (mg g^{-1}), C_e the equilibrium concentration of MG (mg L^{-1}), K_F (mg g^{-1} (L mg^{-1})$^{1/n}$) the Freundlich adsorption constant, and 1/n (unitless) a measure of adsorption intensity. K_F and 1/n are also related to the magnitude of the adsorption driving force and the distribution of the energy sites on the adsorbent.[39]

All the experimental adsorption isotherms were well fitted by the Freundlich equation (Fig. 3A). Table 1 summarizes the obtained Freundlich parameters. The values of K_F and adsorption capacity increased with adsorption temperature, indicating that the adsorption of MG on MIL-100(Fe) is endothermic. The values of 1/n are less than 1 (0.579 to 0.809) in the adsorption temperature range of 25–50 °C, suggesting that MIL-100(Fe) possesses heterogeneous surface caused by the presence of different functional groups on the surface.[34,40] The lack of plateau in desorption isotherms indicates multi-layer adsorption and higher adsorption capacity.

Thermodynamics for the adsorption of MG on MIL-100(Fe)

To get further insight into the adsorption mechanism, the thermodynamic parameters, standard free energy change (ΔG^0, kJ mol^{-1}), enthalpy change (ΔH^0, KJ mol^{-1}) and entropy change (ΔS^0, J mol^{-1} K^{-1}) for the adsorption of MG on MIL-100(Fe) were determined based on eqn (2)–(4):

$$K_0 = \frac{C_s}{C_e} \quad (2)$$

$$\Delta G^0 = -RT\ln K_0 \quad (3)$$

$$\ln K_0 = \frac{\Delta S^0}{R} - \frac{\Delta H^0}{RT} \quad (4)$$

where K_0 is the adsorption equilibrium constant, C_s the amount of MG adsorbed per mass of MIL-100(Fe) (mg g^{-1}), C_e the MG concentration in solution at equilibrium (mg L^{-1}), R universal gas constant, and T temperature.

The value of ln K_0 at a certain temperature was obtained by plotting ln(C_s/C_e) against C_s and extrapolating C_s to zero based on eqn (2) (Fig. S2, ESI†),[41] while those of ΔH^0 and ΔS^0 were determined by plotting ln K_0 against 1/T (Fig. S3, ESI†) based on eqn (3). The determined values of ln K_0, ΔG^0, ΔH^0 and ΔS^0 are given in Table 1. Negative ΔG^0 means spontaneous adsorption of MG on MIL-100(Fe) in the temperature range studied. The positive ΔH^0, which is supported by increased adsorption capacity of MG at high temperatures, suggests that the adsorption of MG on MIL-100(Fe) is endothermic (Table 1). The positive ΔH^0 is unfavorable for spontaneous adsorption of MG on MIL-100(Fe). However, positive ΔS^0 is favorable for spontaneous adsorption of MG on MIL-100(Fe), which may result from the release of more water molecules desolvated from one MG molecule after adsorption on MIL-100(Fe). Therefore, the driving force for the adsorption of MG on MIL-100(Fe) is controlled by an entropy effect rather than an enthalpy change.

Kinetics for the adsorption of MG on MIL-100

The time-dependent adsorption capacity was obtained to study the kinetics for the adsorption of MG on MIL-100(Fe) (Fig. 4). The adsorption capacity of MG increased significantly in the first 2 h, and reached equilibrium gradually. Moreover, the

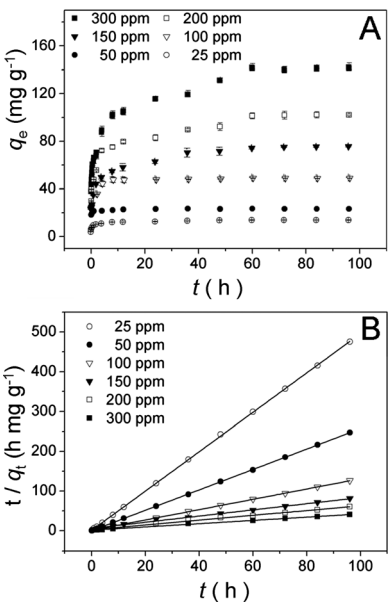

Fig. 4 (A) Effect of contact time on the adsorption of MG on MIL-100(Fe) (10 mg) at different initial concentrations of MG at 30 °C and pH 5.0 and (B) plots of pseudo-second-order kinetics for the adsorption of MG on MIL-100(Fe) (10 mg).

Table 2 Kinetic parameters for the adsorption of MG on MIL-100(Fe) at 30 °C[a]

		Pseudo-second-order kinetic model			Intraparticle diffusion model		
C_0/mg L^{-1}	$q_{e(exp)}$/mg g^{-1}	$q_{e(cal)}$/mg g^{-1}	k_2/g mg^{-1} min^{-1}	R^2	I	k_{i1}/mg g^{-1} min$^{-0.5}$	R^2
25	12.1	12.1	6.67×10^{-3}	1.000	8.16	0.061	0.709
50	23.3	23.4	4.92×10^{-3}	1.000	20.0	0.056	0.890
100	45.8	44.8	3.37×10^{-4}	0.999	38.8	0.12	0.868
150	70.8	77.2	2.79×10^{-5}	0.994	44.5	0.38	0.922
200	95.4	99.6	4.71×10^{-5}	0.994	41.6	0.83	0.981
300	141	146	3.21×10^{-5}	0.997	55.0	1.32	0.922

[a] Notes: C_0, initial concentration of MG; $q_{e(cal)}$, calculated adsorption capacity; $q_{e(exp)}$, experimental adsorption capacity; k_2, pseudo-second-order kinetic constant; k_{i1}, intraparticle diffusion rate constant for the first linear portion; and I, intercept for the first linear portion.

adsorption capacity significantly increased as the initial concentration of MG increased, indicating the favorable adsorption at high concentrations of MG. The time dependence for the adsorption of MG on MIL-100(Fe) is well described by a versatile pseudo-second-order kinetic model which is based on the adsorption capacity on the solid phase and is in agreement with a chemisorption mechanism being the rate controlling step (eqn (5)):[29]

$$\frac{t}{q_t} = \frac{1}{k_2 q_e^2} + \frac{1}{q_e} t \quad (5)$$

where q_e and q_t are the adsorption capacity (mg g^{-1}) at equilibrium and at any time t (min), respectively, k_2 the rate constant for pseudo-second-order adsorption (g mg^{-1} min^{-1}). The plots of t/q_t against t constructed from Fig. 4A gave straight lines (Fig. 4B), and the values of q_e and k_2 were determined from the slopes and intercepts of the plots (Table 2). The equilibrium adsorption capacity q_e increased from 12.1 to 146 mg g^{-1} as initial concentration varied from 25 to 300 mg L^{-1}. Moreover, the rate constant k_2 decreased as the initial MG concentration increased, indicating that chemisorption was significant in the rate-limiting step, involving valency forces through sharing or exchange of electrons between MG and MIL-100(Fe).[42] This mechanism was supported by the XPS spectra showing the shift of the N 1s peak of the MG and the Fe 2p peak in MIL-100(Fe) after the adsorption of MG on MIL-100(Fe) (Fig. 5).

The XPS spectra show that the adsorption of MG on MIL-100(Fe) led to a shift to higher energy for the N 1s peak of the MG (from 399.3 eV to 400.2 eV), a shift to lower energy for the Fe 2p peak in MIL-100(Fe) (from 725.3 eV and 711.7 eV to 724.9 eV and 711.2 eV, respectively) (Fig. 5). Although the open metal sites in MIL-100(Fe) have been occupied by water molecules through the coordination in aqueous solution, the water molecules can still be replaced by other stronger Lewis bases. Thus, the interaction between the Lewis base –N(CH$_3$)$_2$ in MG and the Lewis acid Fe sites of MIL-100(Fe) can occur due to the replacement of the water molecules by the Lewis base –N(CH$_3$)$_2$ of MG. MG molecule cannot completely enter the pore of MIL-100(Fe) as the pore window is smaller than the size of MG molecule. However, the MG molecule can partially enter the pore of MIL-100(Fe) as the pore window is large enough for its –N(CH$_3$)$_2$ and –C$_6$H$_5$ groups (Fig. 6B). Besides, the possibility to

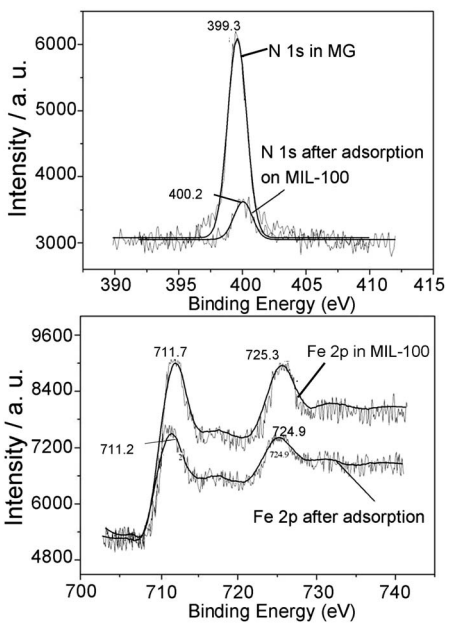

Fig. 5 XPS spectra of: (A) N 1s in pure MG and adsorbed on MIL-100(Fe) and (B) Fe 2p in MIL-100 and after adsorption of MG on surface of MIL-100(Fe).

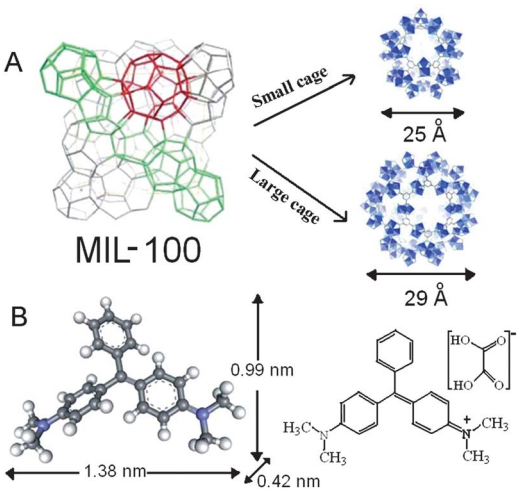

Fig. 6 (A) Structure of MIL-100(Fe). Adapted and reproduced with permission from ref. 35. Copyright 2007 Royal Society of Chemistry; (B) structure of MG simulated with ChemBioOffice 2008 (Cambridge Soft Corporation). Molecular kinetic diameters were approximated using the minimum cross-sectional area and molecular properties and parameters listed in Table S1†.

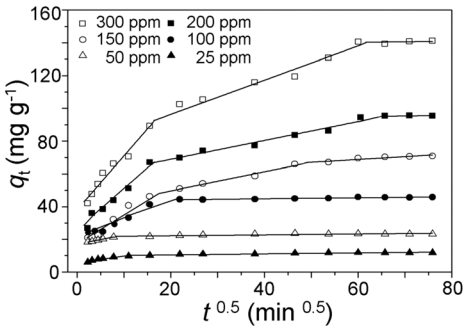

Fig. 7 Intraparticle diffusion plot for the adsorption of MG on MIL-100(Fe) (10 mg) with different initial concentrations of MG at 30 °C and pH 5.0. Error bars, in most cases smaller than the symbols, represent standard deviations.

establish π–π interaction between the benzene rings in MG and MIL-100(Fe) may also play important roles (Fig. 6).

The kinetic data were further analyzed with the intraparticle diffusion model (eqn (6)) to elucidate if the diffusion mechanism was involved in the adsorption of MG on MIL-100(Fe):

$$q_t = k_i t^{0.5} + I \quad (6)$$

where q_t (mg g^{-1}) is the adsorption capacity at time t, k_i (mg g^{-1} min$^{-0.5}$) the intraparticle diffusion rate constant, and I the intercept. The k_i value can be found from the slope of q_t against $t^{0.5}$ plot. If the value of I is zero, then the rate of adsorption is controlled by intraparticle diffusion for the entire adsorption period.[43] However, the plot of q_t against $t^{0.5}$ shows multilinear portions (Fig. 7), suggesting that more than one process affected the adsorption.[44]

The values of the slopes of q_t against $t^{0.5}$ plots are not zero, implying that film (boundary layer) diffusion controlled the adsorption rate at the beginning.[45] The multiple nature observed in the intraparticle diffusion plots suggests that intraparticle diffusion is not solely rate-limiting step.[46]

Comparison of MIL-100(Fe) with other adsorbents for the adsorption of MG

The adsorption isotherms of the MG on MIL-101(Cr), MIL-53(Al) and activated carbon were also studied for comparison (Fig. 3B). The characteristic data and structures of these adsorbents for MG are shown in Fig. 6, Table S2 and Fig. S4 (ESI†). MIL-100(Fe), MIL-101(Cr) and MIL-53(Al) gave significantly larger specific surface area and total pore volume than activated carbon, but only MIL-100(Fe) offered much higher adsorption capacity for MG than activated carbon as MG can be strongly adsorbed on the surface of MIL-100(Fe) *via* surface complexation and electrostatic interactions between cationic MG and negatively charged MIL-100(Fe). The larger surface area of MIL-100(Fe) produced more active adsorption site than MIL-53(Al) and activated carbon. Furthermore, MIL-100(Fe) provided water molecule coordinated metal centers (Fe^{3+}) to interact with Lewis acid–base sites of MG, whereas MIL-53(Al) had no such metal sites (Table S2, ESI†).

The surface positive charge of MIL-101(Cr) below pH 10 (Fig. S5, ESI†) led to lower adsorption capacity for MG due to the electrostatic repulsion between the surface of MIL-101(Cr) and MG though MIL-101(Cr) also has water molecule coordinated metal sites and even larger pore and surface area than MIL-100(Fe). Meanwhile, the adsorption capacity of MIL-100(Fe) is higher than MIL-53(Al), indicating that the water molecule coordinated metal sites played an important role in adsorption. Activated carbon has lower adsorption capacity than MIL-100(Fe), and is easy to reach saturation capacity. However, saturation has not been reached in the adsorption isotherm of MG on MIL-100(Fe), indicating that MIL-100 has the potential for even much higher adsorption capacity. The adsorption capacity of MIL-100(Fe) for MG is much higher than those of other adsorbents such as MIL-53(Al), activated carbon, natural zeolite, and chitosan bead (Fig. 3B; Table S3, ESI†).

Desorption and regeneration of MIL-100(Fe)

Desorption and regeneration of MG-loaded MIL-100(Fe) were achieved using ethanol solution (including 0.5% HCl) with a higher desorption efficiency of 97.3% (Fig. S6, ESI†). The framework of MIL-100(Fe) remained stable after regeneration with the solutions of salt, acid and ethanol under ultrasound assisted desorption (Fig. S7, ESI†). The good reusability of spent MIL-100(Fe) (Fig. S8, ESI†) also demonstrates the potential of MIL-100(Fe) for the adsorption and removal of MG.

Conclusions

We have reported the adsorption of malachite green from aqueous solution on a highly porous metal–organic framework MIL-100(Fe) in view of the adsorption isotherm, thermodynamics, kinetics, and regeneration of the sorbent. The high adsorption capacity, good solvent stability, and excellent reusability make MIL-100(Fe) promising as a novel adsorbent for the adsorption and removal of MG from aqueous solution.

Acknowledgements

This work was supported by the National Natural Science Foundation of China (Grants 20935001 and 21077057), and the Fundamental Research Funds for the Central Universities.

References

1 O. M. Yaghi, M. O'Keeffe, N. W. Ockwig, H. K. Chae, M. Eddaoudi and J. Kim, *Nature*, 2003, **423**, 705.
2 S. Kitagawa, R. Kitaura and S. Noro, *Angew. Chem., Int. Ed.*, 2004, **43**, 2334.
3 M. Eddaoudi, D. B. Moler, H. L. Li, B. L. Chen, T. M. Reineke, M. O'Keeffe and O. M. Yaghi, *Acc. Chem. Res.*, 2001, **34**, 319.
4 G. Férey, *Chem. Soc. Rev.*, 2008, **37**, 191.
5 J. R. Li, R. J. Kuppler and H.-C. Zhou, *Chem. Soc. Rev.*, 2009, **38**, 1477.
6 K. A. Cychosz, R. Ahmad and A. J. Matzger, *Chem. Sci.*, 2010, **1**, 293.
7 J. R. Li, J. Sculley and H.-C. Zhou, *Chem. Rev.*, 2012, **112**, 869.
8 M. P. Suh, H. J. Park, T. K. Prasad and D.-W. Lim, *Chem. Rev.*, 2012, **112**, 782.
9 K. Sumida, D. L. Rogow, J. A. Mason, T. M. McDonald, E. D. Bloch, Z. R. Herm, T.-H. Bae and J. R. Long, *Chem. Rev.*, 2012, **112**, 724.
10 C.-Y. Huang, M. Song, Z.-Y. Gu, H.-F. Wang and X.-P. Yan, *Environ. Sci. Technol.*, 2011, **45**, 4490.

11 S. Galli, N. Masciocchi, V. Colombo, A. Maspero, G. Palmisano, F. J. Lopez-Garzon, M. Domingo-Garcia, I. Fernandez-Morales, E. Barea and J. A. R. Navarro, *Chem. Mater.*, 2010, **22**, 1664.
12 K. A. Cychosz and A. J. Matzger, *Langmuir*, 2010, **26**, 17198.
13 E. Haque, J. W. Jun and S. H. Jhung, *J. Hazard. Mater.*, 2011, **185**, 507.
14 E. Haque, J. E. Lee, I. T. Jang, Y. K. Hwang, J.-S. Chang, J. Jegal and S. H. Jhung, *J. Hazard. Mater.*, 2010, **181**, 535.
15 M. Maes, F. Vermoortele, L. Alaerts, J. F. M. Denayer and D. E. De Vos, *J. Phys. Chem. C*, 2011, **115**, 1051.
16 M. Maes, S. Schouteden, L. Alaerts, D. Depla and D. E. De Vos, *Phys. Chem. Chem. Phys.*, 2011, **13**, 5587.
17 E. Haque, J. W. Jun, S. N. Talapaneni, A. Vinu and S. H. Jhung, *J. Mater. Chem.*, 2010, **20**, 10801.
18 S. H. Jhung, J.-H. Lee, J. W. Yoon, C. Serre, G. Férey and J.-S. Chang, *Adv. Mater.*, 2007, **19**, 121.
19 K. A. Cychosz, A. G. Wong-Foy and A. J. Matzger, *J. Am. Chem. Soc.*, 2008, **130**, 6938.
20 S. Achmann, G. Hagen, M. Hämmerle, I. Malkowsky, C. Kiener and R. Moos, *Chem. Eng. Technol.*, 2010, **33**, 275.
21 G. Blanco-Brieva, J. M. Campos-Martin, S. M. Al-Zahrani and J. L. G. Fierro, *Fuel*, 2011, **90**, 190.
22 K. A. Cychosz, A. G. Wong-Foy and A. J. Matzger, *J. Am. Chem. Soc.*, 2009, **131**, 14538.
23 T. Robinson, G. McMullan, R. Marchant and P. Nigam, *Bioresour. Technol.*, 2001, **77**, 247.
24 P. Janoš, *Environ. Sci. Technol.*, 2003, **37**, 5792.
25 S. J. Culp and F. A. Beland, *J. Am. Coll. Toxicol.*, 1996, **15**, 219.
26 S. Srivastava, R. Sinha and D. Roy, *Aquat. Toxicol.*, 2004, **66**, 319.
27 M. M. Cheng, W. H. Ma, J. Li, Y. P. Huang, J. C. Zhao, Y. X. Wen and Y. M. Xu, *Environ. Sci. Technol.*, 2004, **38**, 1569.
28 C. J. Cha, D. R. Doerge and C. E. Cerniglia, *Appl. Environ. Microbiol.*, 2001, **67**, 4358.
29 G. Crini, H. N. Peindy, F. Gimbert and C. Robert, *Sep. Purif. Technol.*, 2007, **53**, 97.
30 C. Akmil-Başar, Y. Önal, T. Kılıçer and D. Eren, *J. Hazard. Mater.*, 2005, **127**, 73.
31 T. Santhi, S. Manonmani and T. Smitha, *J. Hazard. Mater.*, 2010, **179**, 178.
32 R. P. Han, Y. Wang, Q. Sun, L. L. Wang, J. Y. Song, X. T. He and C. C. Dou, *J. Hazard. Mater.*, 2010, **175**, 1056.
33 G. Atun, G. Hisarlı, A. E. Kurtoğlu and N. Ayar, *J. Hazard. Mater.*, 2011, **187**, 562.
34 B. H. Hameed and M. I. El-Khaiary, *J. Hazard. Mater.*, 2008, **157**, 344.
35 P. Horcajada, S. Surblé, C. Serre, D.-Y. Hong, Y.-K. Seo, J.-S. Chang, J.-M. Grenèche, I. Margiolaki and G. Férey, *Chem. Commun.*, 2007, 2820.
36 J. W. Yoon, Y.-K. Seo, Y. K. Hwang, J.-S. Chang, H. Leclerc, S. Wuttke, P. Bazin, A. Vimont, M. Daturi, E. Bloch, P. L. Llewellyn, C. Serre, P. Horcajada, J.-M. Grenèche, A. E. Rodrigues and G. Férey, *Angew. Chem., Int. Ed.*, 2010, **49**, 5949.
37 I. D. Mall, V. C. Srivastava, N. K. Agarwal and I. M. Mishra, *Colloids Surf., A*, 2005, **264**, 17.
38 I. D. Mall, V. C. Srivastava, G. V. A. Kumar and I. M. Mishra, *Colloids Surf., A*, 2006, **278**, 175.
39 C.-L. Hsueh, Y.-W. Lu, C.-C. Hung, Y.-H. Huang and C.-Y. Chen, *Dyes Pigm.*, 2007, **75**, 130.
40 F. Haghseresht and G. Q. Lu, *Energy Fuels*, 1998, **12**, 1100.
41 Y. H. Li, Z. C. Di, J. Ding, D. H. Wu, Z. K. Luan and Y. Q. Zhu, *Water Res.*, 2005, **39**, 605.
42 Y. S. Ho and G. McKay, *Process Biochem.*, 1999, **34**, 451.
43 V. Vadivelan and K. V. Kumar, *J. Colloid Interface Sci.*, 2005, **286**, 90.
44 E. Bulut, M. Ozacar and I. A. Sengil, *Microporous Mesoporous Mater.*, 2008, **115**, 234.
45 L. Wang, J. Zhang, R. Zhao, C. Li, Y. Li and C. L. Zhang, *Desalination*, 2010, **254**, 68.
46 V. J. P. Poots, G. McKay and J. J. Healy, *J. - Water Pollut. Control Fed.*, 1978, **50**, 926.